Decellularized pulp matrix as scaffold for mesenchymal stem cell mediated bone regeneration

Dong Joon Lee[1] iD, Patricia Miguez[1,2], Jane Kwon[1,3], Renie Daniel[4], Ricardo Padilla[5], Samuel Min[1], Rahim Zalal[1], Ching-Chang Ko[6] and Hae Won Shin[3] iD

Abstract

Scaffolds that are used for bone repair should provide an adequate environment for biomineralization by mesenchymal stem cells (MSCs). Recently, decellularized pulp matrices (DPM) have been utilized in endodontics for their high regenerative potential. Inspired by the dystrophic calcification on the pulp matrix known as pulp stone, we developed acellular pulp bioscaffolds and examined their potential in facilitating MSCs mineralization for bone defect repair. Pulp was decellularized, then retention of its structural integrity was confirmed by histological, mechanical, and biochemical evaluations. MSCs were seeded and proliferation, osteogenic gene expression, and biomineralization were assessed to verify DPM's osteogenic effects in vitro. MicroCT, energy-dispersive X-ray (EDX), and histological analyses were used to confirm that DPM seeded with MSCs result in greater mineralization on rat critical-sized defects than that without MSCs. Overall, our study proves DPM's potential to serve as a scaffolding material for MSC-mediated bone regeneration for future craniofacial bone tissue engineering.

Keywords

Decellularized pulp matrix, dystrophic calcification, mesenchymal stem cells, critical sized defect, biomineralization

Received: 13 September 2020; accepted: 28 November 2020

Introduction

Critical sized defects (CSD) in bones can be caused by trauma, tumor, nonunion fractures, degeneration, or congenital deformities, and require surgical intervention with template scaffolding material to repair. Many bone substitute biomaterials including bioactive ceramics, bioactive glasses, biological or synthetic polymers, and composites materials have been introduced as alternatives of autografts or allografts, which have been considered clinical gold standards in grafts for many years.[1,2] Over time, the paradigm of grafting materials shifted toward tissue engineered graft to enhance tissue regeneration.[3] The advancement in bone tissue engineering (TE) has enabled the development of constructs consisting of mesenchymal stem cells (MSCs) and biomaterials, which are now considered a potential bone grafting option that can replace autograft and allograft.[4,5] However, to date, the optimal

[1]Oral and Craniofacial Health Science Institute, School of Dentistry, University of North Carolina, Chapel Hill, NC, USA
[2]Department of Periodontics, School of Dentistry, University of North Carolina, Chapel Hill, NC, USA
[3]Department of Neurology and Neurosurgery, School of Medicine, University of North Carolina, Chapel Hill, NC, USA
[4]Department of Oral and Maxillofacial Surgery, School of Dentistry, University of North Carolina, Chapel Hill, NC, USA
[5]Department of Diagnostic Sciences, School of Dentistry, University of North Carolina, Chapel Hill, NC, USA
[6]Department of Orthodontics, School of Dentistry, University of North Carolina, Chapel Hill, NC, USA

Corresponding author:
Hae Won Shin, Department of Neurology and Neurosuregry, School of Medicine, University of North Carolina, CB #7454, 101 manning drive, Campus Box #7025, Chapel Hill, NC 27599, USA.
Email: shinhw@neurology.unc.edu

scaffold for bone regeneration has yet to be defined. Thus, it is necessary to find the most appropriate scaffold that can provide optimal environment for cellular delivery and biomineralization by the MSCs.

In the past years, the application of natural scaffolds prepared by decellularization has gained popularity in bone TE applications.[6,7] The decellularization process has been proved effective in not only removing antigenic cellular components, but also preserving the native 3D architectural support and composition of the extracellular matrix (ECM) of the specific tissue. Previously, bone tissue was decellularized and seeded with cells in an attempt to evaluate its potential as a scaffold for bone regeneration. The study revealed that while decellularized bone matrix (DecBM) shows a high osteogenic differentiation potential in vitro and osteoconduction in vivo, its application as a 3D bone scaffold is inadequate due to its limitation in inducing cellular infiltration into the compact mineralized matrix, and made it necessary to look into other substitute tissue sources.[8] In the field of dentistry, recent endodontic studies discovered human dental pulp's regenerative potential by using decellularization techniques utilizing it as a scaffold for pulp regeneration.[9] Hu et al. also reported that pulps from swine can be decellularized and that it is feasible to use them as xenogenic bioscaffolds for improving clinical outcomes and functions by regenerating human dental pulp.[10]

Dental pulp is a highly vascularized small organ located in the pulp cavity of each tooth. Pulp ECM is composed of type I and III collagen fibrils, which contribute to the architectural support, glycosaminoglycan, proteoglycan, and non-collagenous proteins such as fibronectin, vitronectin, osteopontin, and bone sialoprotein. The ECM also contains growth factors, including transforming growth factor β-1 (TGFβ-1), TGFβ-3, bone morphogenetic protein-2 (BMP-2), insulin-like growth factor-1 (IGF-1), and vascular endothelial growth factor (VEGF), which are key proteins for cell differentiation and matrix mineralization.[11–14] Dental pulp is interfaced with an environment where continuous mineralized tissue, dentin, repair is required. Although odontoblasts are known to be the key player in dentin regeneration, the surrounding matrix may also have an influence on hard tissue regeneration. Current clinical challenges in regenerative endodontic procedure is acquiring rather bone-like tissue containing connective tissue than the pulp-dentin complex. Revascularization promoting cell homing is considered for the reason of ectopic mineralized tissue formation.[15] Occasionally, a dystrophic calcification occurs on the pulp tissue, of which the condition is known as pulp stone. In pulp stones, the calcification grows in size by addition of collagen fibrils to their surface or by calcification of pre-existing collagen fibres.[11] The precise etiology for calcification is unknown, but it is speculated that pulp mesenchymal cells are induced by growth factors leading to odontogenesis.[16]

A recent report observed that the silk fibroin scaffold with decellularized pulp was better at inducing new bone formation and vascularization in rabbit calvaria than the scaffolds without decellularized pulp.[14,17,18] Inspired by the above evidences of pulp calcification and calvaria bone regeneration using decellularized pulp matrices (DPM) effect, we investigated the potential of DPM as a promising bone scaffolding material with advantageous qualities that sufficiently address the limitations of the decellularized bone. Currently, few decellularization protocols exist only for regenerative endodontics, and no studies have reported utilization of DPM for bone regeneration alone or with cells. Our study is both novel and promising in developing new biological scaffold for bone regeneration.

In this study, we prepared a decellularized dental pulp and tested its feasibility as a scaffold material for tissue-engineered bone regeneration. After the optimization of the procedure for the decellularization of pulp, proliferative and osteogenic effects of the DPM on MSCs were assessed in vitro. Then, in vivo bone formation was evaluated using CSD in rat calvaria model (Figure 1). Unique 3D microenvironment of pulp matrix was hypothesized to facilitate hydroxyapatite deposition on their collagen matrix with the assistance of osteogenically differentiated MSCs. Overall, the study explored decellularized pulp's potential as an alternative natural bone scaffold in future bone TE application.

Materials and methods

Decellularization of dental pulp

Discarded impacted human third molars ($n = 40$) were obtained from the clinic (14–40 years old). Freshly extracted molars were immediately placed in 1x Hanks' Balanced Salt solution (HBSS) with 2% penicillin and streptomycin and stored at 4°C until they were processed for no longer than 3 h. Under sterile condition, the pulp chamber was exposed using dental bur, and pulp removed and washed in dH$_2$O for 1 h. Using 1% Triton X-100 (Sigma–Aldrich, St Louis, MO, USA) and 0.1% ammonium hydroxide (Sigma–Aldrich, St Louis, MO, USA), pulps were decellularized on a shaker at 4°C. The solution was replaced every 24 h for 7 days. After being washed with dH$_2$O, pulp was lyophilized and sterilized using ethylene oxide gas. To test in vitro effects on MSCs, whole DPM were frozen in liquid nitrogen and mechanically pulverized. Powdered DPM (40 mg) was added in each well of 12 well-plate with MSC. To test for acellularity, DNA was isolated from DPM and natural pulp matrix (NPM, cellularized and intact) using QIAamp tissue kit (Qiagen, Hilden, Germany) and visualized by performing agarose gel (1%) electrophoresis. DNA content from pulp (20 mg) was measured with NanoDrop™ 2000 spectrophotometers (Thermo Scientific, Waltham, IL, USA). Both whole DPM
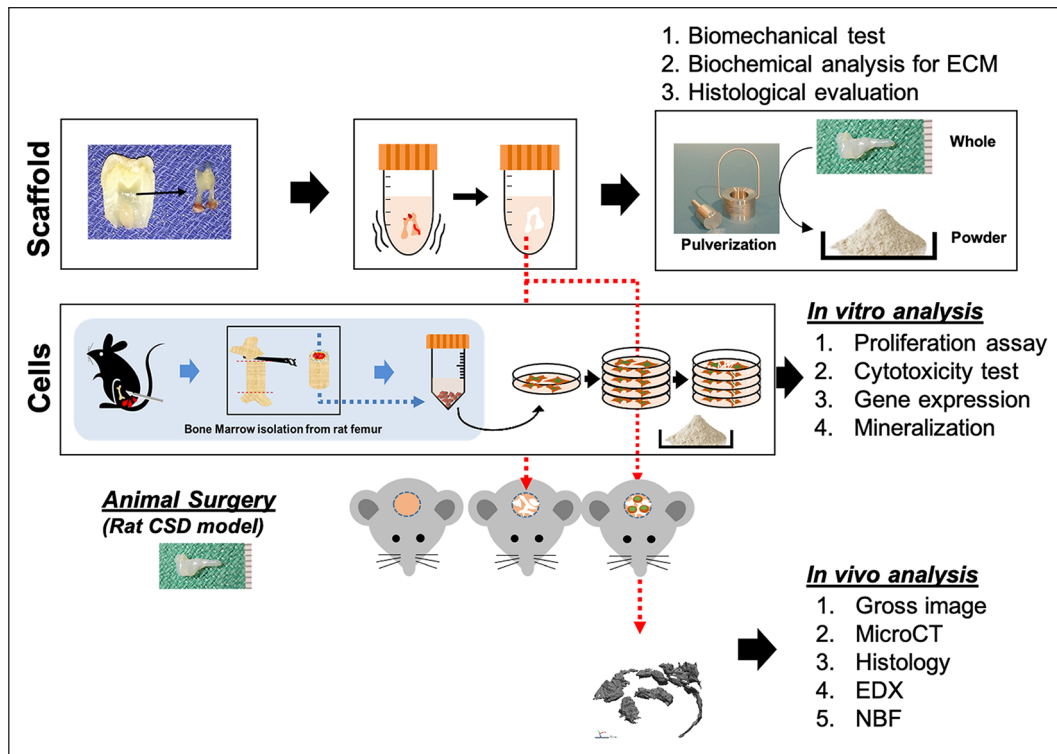
Figure 1. Schematic of the study. Pulps isolated from third molars were decellularized to prepare DPM. MSCs isolated from the rat femur were seeded with DPM and implanted on the rat CSD.

and NPM were fixed for 2 days in 10% neutral formalin solution, embedded in freezing medium (Sakura Finetek, Torrance, CA, USA), sectioned into 5 μm slices using a Cryotome (Leica Biosystems CM3050 S, Richmond, IL, USA), and stained with hematoxylin and eosin (H&E), Masson's Trichrome, and DAPI staining.

Scanning electron microscopy (SEM) and energy-dispersive X-ray spectroscopy (EDX) analysis

Whole NPM and DPM were fixed in a cacodylate/saccharose buffer solution (0.05 M/0.6 M; pH 7.4) for 2 h at room temperature, before critical point-drying. Samples were then sputter-coated with platinum in a vacuum and imaged with SEM (Model S-2256N; Hitachi High Technologies America, Inc., Schaumburg, IL, USA). Minerals formed by DPM were analyzed using an EDX microanalysis microprobe fitted to the SEM. The analysis was performed at least three random regions on each area in the CSD, which were analyzed by INCA operator software (Oxford Instruments Analytical, High Wycombe, UK). Calcium/phosphate ratio (Ca:P) was calculated from the peaks in the EDX pattern.

Biomechanical and biochemical test

Whole DPM and NPM were stored in PBS until the tensile-stress test was performed. Each group ($n = 5$) was tested using Dynamic Mechanical Analysis (TA Instruments, New Castle, DE, USA). Samples were clamped and stretched to tensile failure at a rate of 10 mm/min. Failure point and ultimate stress was then determined from the stress–strain curves.

For soluble protein quantification, protein from DPM and NPM (20 mg) powders were lysed using RIPA buffer containing protease inhibitor (Thermo Scientific, Waltham, IL, USA) and extracted, then measured using Pierce BCA Protein Assay Kit (Thermo Scientific, Waltham, IL, USA) at 560 nm and calculated based on the BSA standard curve. Total collagen content was quantified based on free Hydroxyproline content after acid hydrolysis of samples, using a total collagen assay kit (Abcam, Cambridge, MA, USA) followed by the company's instruction. Both DPM ($n = 5$) and NPM ($n = 5$) were hydrolyzed with 10 N hydrochloric acid at 120°C for 1 h and neutralized with 10 N sodium hydroxide. Then, the absorbance was measured at 560 nm (BioRad, Hercules, CA, USA). The total collagen contents were calculated (μg/mg) based on the standard rat tail collagen samples included in the assay kit.

VEGF measurement

VEGF was quantified from 20 mg of using an enzyme-linked immunosorbent assay (ELISA) kit (Thermo Scientific, Waltham, IL, USA). Briefly, the pulverized DPM and NPM were dissolved in 1 ml RIPA buffer

(150 mM NaCl, 50 mM Tris, 1% TX-100, 0.5% sodium deoxycholate, 0.1% sodium dodecyl sulfate). Lysates were sonicated for 30 s, incubated for 12 h at 4°C on a shaker and centrifuged at 13,000g for 10 min. The concentration of vascular endothelial growth factor (VEGF) concentration was determined by ELISA. The VEGF kit was used according to the manufacturer's instructions. Absorbance was measured at 650 nm. Experiments were replicated three times. Data was represented as pg/ml of total tissues, in each group.

MSCs isolation and characterization

MSCs were isolated as described in the previous study.[19] Briefly, male Sprague-Dawley (SD) rats (Charles River; about 250–300 g, 6 weeks old), were sacrificed; their femurs were removed, and the bone marrow was flushed out using a 20-gauge needle. Cells from the marrow were seeded in 100-mm culture dish using Dulbecco's Modified Eagle's Medium-Low Glucose (Sigma–Aldrich, St Louis, MO, USA) supplemented with 10% fetal bovine serum (Hyclone Laboratories Inc., Logan, UT, USA). Culture dishes were incubated at 37°C in 5% CO_2. After 24 h, adherent cells were continually cultured. Fresh medium was replaced every 3 days. All experiments were performed using MSCs at passage 5.

Live and dead viability test

To examine the toxic effect of DPM on MSCs, Live/Dead Assay was performed using a commercial kit (Molecular Probes, Eugene, OR, USA). MSCs were cultured on a 35-mm dish with the addition of DPM powder for 3 days. Green fluorescence positive MSCs by calcein and red fluorescence positive by ethidium homodimer-1 were imaged at 10 randomly selected areas and quantified using Image J software.[20]

Proliferation assay

MSCs with DPM powder were plated in 12-well plates at a density of 50,000 cells per well and cultured for 1, 3, 5, and 7 days. MSCs without DPM powder served as a control group. MTS (3-(4,5-dimethylthiazol-2-yl)-5-(3-carboxymethoxyphenyl)-2-(4-sulfophenyl)-2-Htetrazolium) Cell Proliferation Assay Kit (Promega Co., Madison, WI, USA) was used to measure optical density of MTS solution reacted with MSCs on the days according to company instructions.

Osteogenic gene expression

Total RNAs were extracted using Trizol reagent (Invitrogen, Carlsbad, CA, USA). Then, complementary DNA was synthesized using iScript Kit (BioRad) and

Table 1. Primers used in this study for real–time polymerase chain reaction (PCR) to measure osteogenic gene expression.

Target	Primer sequence (5′-3′)
Runx2	F: CCTGAACTCAGCACCAAGTCCT
	R: TCAGAGGTGGCAGTGTCATCA
OSX	F: CCGGCCACGCTACTTTCTT
	R: TGGACTGGAAACCGTTTCAGA
OCN	F: CTGACCTCACAGATGCCAA
	R: GGTCTGATAGTCTGTCACAA
ALP	F: AACCCAGACACAAGCATTCC
	R: GCCTTTGAGGTTTTTGGTCA
Col1a2	5′-TCCGGCTCCTGCTCCTCTTA-3′
	5′-GGCCAGTGTCTCCCTTG-3′
GAPDH	F: TGAGGTGACCGCATCTTCTTG
	R: TGGTAACCAGGCGTCCGATA

ALP: alkaline phosphatase; Col1a2: and GAPDH: glyceraldehyde 3-phosphate dehydrogenase; Runx2, OSX, OCN: osteocalcin.

utilized for real-time polymerase chain reaction (PCR) with the 7200 Fast Real-Time PCR System (Applied Biosystems) to determine messenger RNA expression of each osteogenic-specific gene. PCR amplifications were performed using specific primers (Invitrogen, Carlsbad, CA, USA) for Runx2, ALP, COL, OSX, and OCN genes (Table 1). All probes used to detect target genes were labeled with SYGR (BioRad, Hercules, CA, USA). The PCR conditions were run at 94°C for 1 min, followed by 95°C for 30 s, then 58°C for 40 s for a total of 35 cycles. The ΔΔCt method was used to calculate relative levels of gene expression. All reactions were run in triplicate and were normalized to GAPDH.

In vitro mineralization

To analyze mineralization, MSCs were seeded in 12-well culture dishes, 100,000 cells per well with or without DPM powder, with osteogenic media supplied every 3 days. The wells were fixed in 95% ethanol for 30 min at room temperature after 14, 21, and 28 days. Then cells were washed with dH$_2$O and stained with 1% Alizarin Red S (ARS, pH 4.2) for 10 min at room temperature on a shaker, then rinsed three times with dH$_2$O. After complete air-dry, stained plates were imaged using Nikon stereomicroscope (Nikon Instruments Inc., Melville, NY, USA). Quantitative analysis was performed following an extraction with 10% (w/v) cetylpyridinium chloride (CPC) for 30 min at room temperature; the optical density was measured at 570 nm using Gemini SpectraMax Microplate Reader (Molecular Devices LLC, San Jose, CA USA)

In vivo bone regeneration

Sterilized whole DPMs were soaked in MSC suspension media and cultured in osteogenic media for 7 days. CSDs

(8 mm) were created on calvaria of six SD rats (6 weeks old). The calvaria were implanted with one of two test groups (DPM seeded with MSCs and DPM only). Rats were sacrificed 12 weeks post-surgery. The calvaria was removed, trimmed, and fixed in 10% formalin for 7 days at 4°C, then stored in 70% isopropyl alcohol at 4°C for further analysis for MicroCT and histological evaluation.

The calvaria were scanned with a Skyscan microCT (Skyscan 1076; Skyscan, Aartselaar, Belgium) to acquire images at 40 kV, 1000 mA, 20 μm in resolution, with a 720 ms integration time. Three dimensional images were reconstructed using ITK-SNAP software. Following the reconstruction, newly formed bones in the CSDs of animals from each group were measured using Geomagic Design X™ (3D Systems Inc., SC, USA) software. The bone volume was represented in mm³.

Explanted calvaria were immediately fixed in 10% neutral formalin solution, and decalcified in 14% EDTA in saline (pH 7.4) for 21 days. Then, tissues were dehydrated, embedded in paraffin, and sectioned. Hematoxylin and eosin and Masson trichrome staining were performed to assess the new bone formation. H&E staining was done in UNC animal pathological core and Masson Trichrome staining was performed using Trichrome Stain kit (HT-15: Sigma-Aldrich, St. Louis, MO USA) following by the company instruction. Color images of the histologic sections were acquired using Nikon Eclipse Ti-U camera with automatic stage (Nikon Instruments Inc., Melville, NY USA).

Statistics

Results were represented as mean ± standard deviation after analysis using student's *t*-test and analysis of variance (ANOVA). *p*-values less than 0.05 ($p < 0.05$) were considered statistically significant (*).

Results

Decellularization of human dental pulp

After decellularization with Triton X-100 and NH_4OH for 2 weeks, pulps were successfully converted to acellular matrices. In gross image, the decellularized pulps maintained their original configuration and their color turned to pale white (Figure 2(a)). H&E staining revealed an absence of any residual cells in DPM and a presence of many cells in NBM (Figure 2(e)). The amount of DNA in 25 mg of NPM and DPM was measured using NanoDrop 2000 (Thermo Scientific, Wilmington, DE USA). The DNA content in NPM was 140.7 ± 22.4 ng/mg, while the DNA content in the DecBM group was 7.48 ± 1.36 ng/mg, signifying a significant reduction in the nuclear components (*$p < 0.05$) in the pulp (Figure 2(d)). To visualize the residual DNA after decellularization, gel electrophoresis was performed using 1% agarose gel, which showed no

bands in the DPM group. Conversely, smeared DNA was shown in the NPM group (Figure 2(b)). Figure 2(c) shows a complete removal of cellular DNA, which is indicated by the absence of nuclei staining by 4′,6-diamidino-2-phenylindole (DAPI). H&E, Masson's trichrome staining, and SEM images show the preservation by exposing ECM network (blue: collagen) after decellularization compared to undecellularized natural pulp. SEM exhibited similar matrix orientation and morphology in both NPM and DPM. In NPM, adherent cells were visualized on the matrix, while no cells were visualized in DPM, which was indicative of effective decellularization under the ultrastructural view (Figure 2(e)).

### Mechanical and biochemical assessment for DPM

To test the preservation of structural integrity after decellularization, a tensile testing was conducted using dynamic mechanical analysis (DMA) (TA instruments, New Castle, DE USA). The stress and strain curve showed similar breakdown pattern during uniaxial tensile testing (Figure 3(a)), which indicated that there was no significant differences under the conditions tested. For the NPM and DPM of similar dimensions, the mean failure values of tensile test were 0.04 ± 0.002 MPa and 0.04 ± 0.03 MPa for DPM and NPM, respectively. No significant changes in mechanical strength ($n = 5$, *$p < 0.05$) between the NPM and the DPM indicated that the decellularization process did not have any significant impact on the mechanical strength and preserved ECM's integrity. Our results revealed that fresh NPM can successfully be decellularized without any disruption of its structure and biomechanical properties. Although in the gross view, DPM were visualized to be larger and more swollen than the fresh NPM, there was no significant difference between these samples in tensile strength. Further biochemical quantification of collagen in pulp matrices revealed 8.01 ± 1.88 and 8.22 ± 2.07 μg/mg for NPM and DPM, respectively. There was not much loss on total collagen content after decellularization processes (Figure 3(d)). Conversely, the total soluble proteins in 25 mg of tissue was significantly reduced from NPM to DPM by 89% from 2.25 ± 0.78 to 0.24 ± 0.06 μg/ml after the decellularization process (Figure 3(c)).

Characterization of rat bone marrow derived MSCs

In Figure 4(a), isolated MSCs showed polygonal phenotype by differential interference contrast (DIC) imaging colony-forming capability, and positive expression for CD44 and CD90 antibodies and negative for CD45 and CD34 (data not shown) antibodies in the immunocytochemical analysis. MSCs were also positively stained for
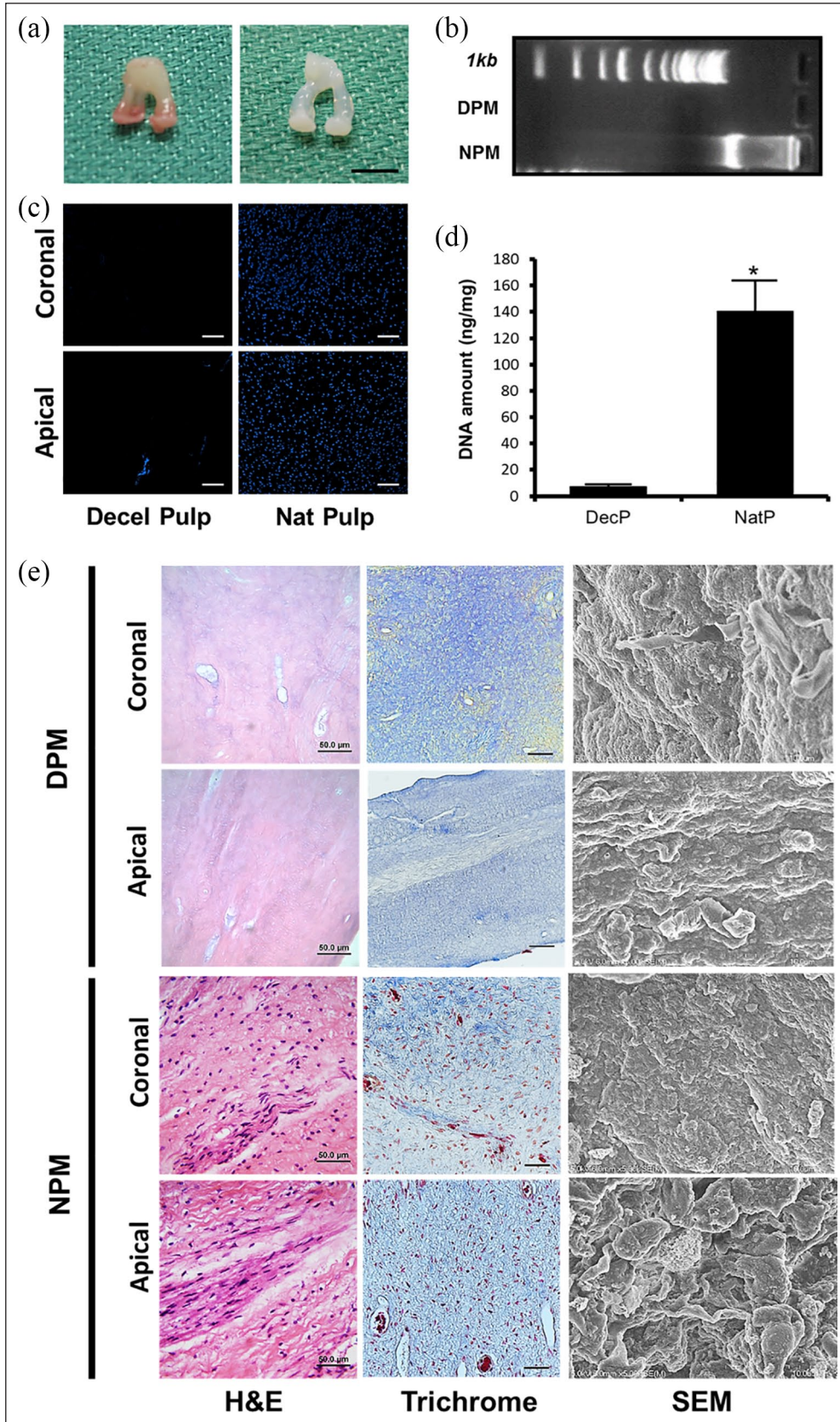
Figure 2. Gross images of decellularized pulp matrix (DPM, a: Left) and natural pulp matrix (NPM, a: Right) (Scale bar 5 mm), DNA analysis to confirm acellularity by agarose gel electrophoresis after decellularization (b), DAPI staining of both coronal and apical region of the natural and decellularized pulp (scale bar: 50 μm) (c), DNA quantification by nanodrop (d), and Histological and scanning electron microscopic (SEM) pictures of the DPM and NPM (e).
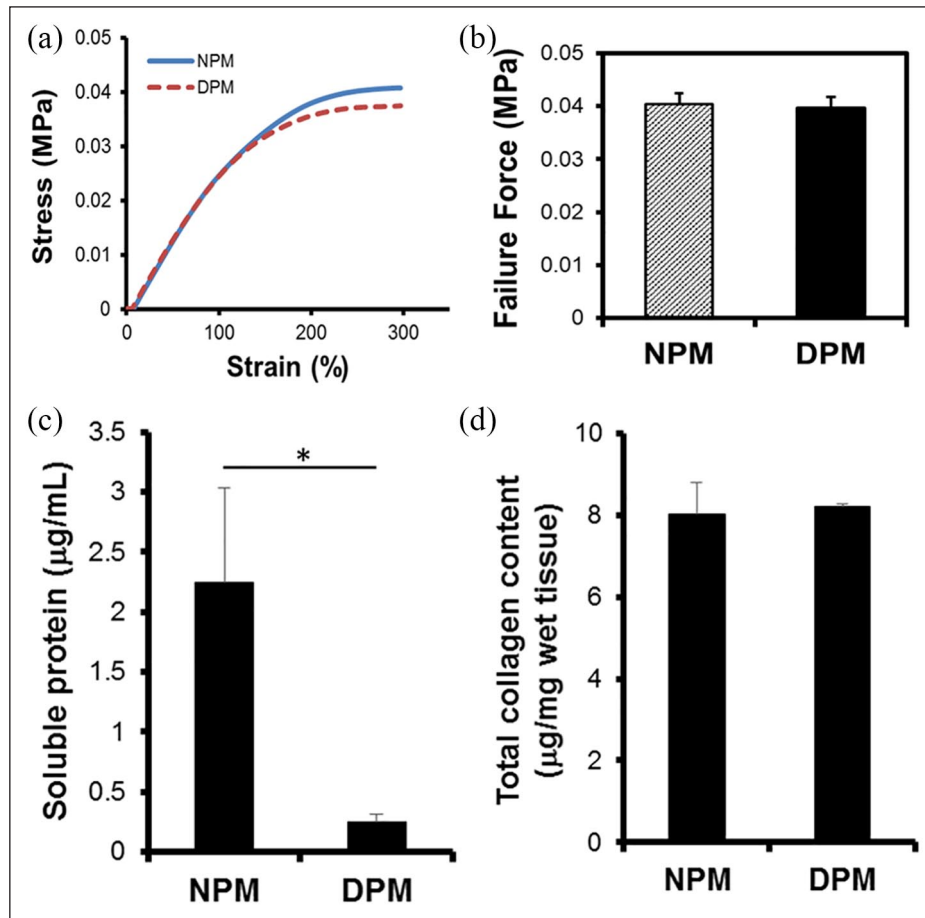
Figure 3. Mechanical and biochemical properties of dental pulp before and after decellularization process. Tensile strength was tested on NPM and DPM ($n = 5$, $*p < 0.05$). Stress-versus-strain analysis (a) and the peak failure force (b) indicated no significant differences between NPM and DPM ($*p > 0.05$). Soluble protein level was significantly decreased ($*p < 0.05$) (c), but total collagen contents remained at a similar level ($*p > 0.05$) after decellularization process.

cartilage-like matrix by Safranin O staining, for lipid vacuoles for Oil Red O staining, and for mineral nodules for Alizarin red S staining after undergoing differentiation under each specific linage induction media. No staining was observed in the control of MSCs in grow media.

### In vitro cytotoxic effect of DPM on MSCs

To evaluate whether the DPM retained any chemical residues that may potentially damage cells, Live/Dead assay was performed. The result showed $91.82 \pm 2.12\%$ live (green) cells and $8.75 \pm 2.63\%$ dead (red) cells in the control group without DPM while the MSC culture with DPM powder showed $79.63 \pm 1.89\%$ live cells and $21.3 \pm 1.54\%$ dead cells (Figure 4(b)).

In vitro osteogenic effects of DPM on proliferation, gene expression, and mineralization

MTS activity was measured on days 1, 3, 5, and 7. Figure 4(c) shows that cellular growth was better with

DPM powders on days 3, 5, and 7 compared to the cell proliferation found in MSCs without DPM. The OD measurements in the MSCs with DPM group on day 3 (0.39 ± 0.02), 5 (0.62 ± 0.05), 7 (0.78 ± 0.04) were higher than that of the MSCs only (control) group (0.33 ± 0.01, 0.51 ± 0.03, and 0.72 ± 0.02, respectively, $*p < 0.05$; Figure 4(c)). This short-term growth results indicated that DPM had stimulatory effects on the MSC proliferation in vitro. Osteogenic gene expression of MSCs culturing with DPM showed a significant increase of ALP (2.84 ± 0.37 folds) gene expression on day 1 in comparison to that (1.64 ± 0.68 folds) without DPM. Runx2 (2.64 ± 0.60 folds), ALP (0.96 ± 0.08 folds), and COL (0.81 ± 0.05 folds) with DPM on day 4 indicated higher gene expression than those (1.47 ± 0.18 folds, 0.59 ± 0.09 folds, and 0.4 ± 0.03 folds) without DPM. On day 14, only APL (1.24 ± 0.24 folds) showed higher gene expression than that (0.78 ± 0.23 folds) with DPM. There were no significant signs of gene expression level in OCN, OPN, Ostrix genes for 7 days (Figure 4(d)). The mineralization of MSCs with or without DPM powder was examined by ARS staining and quantified by CPC extraction of the ARS dye
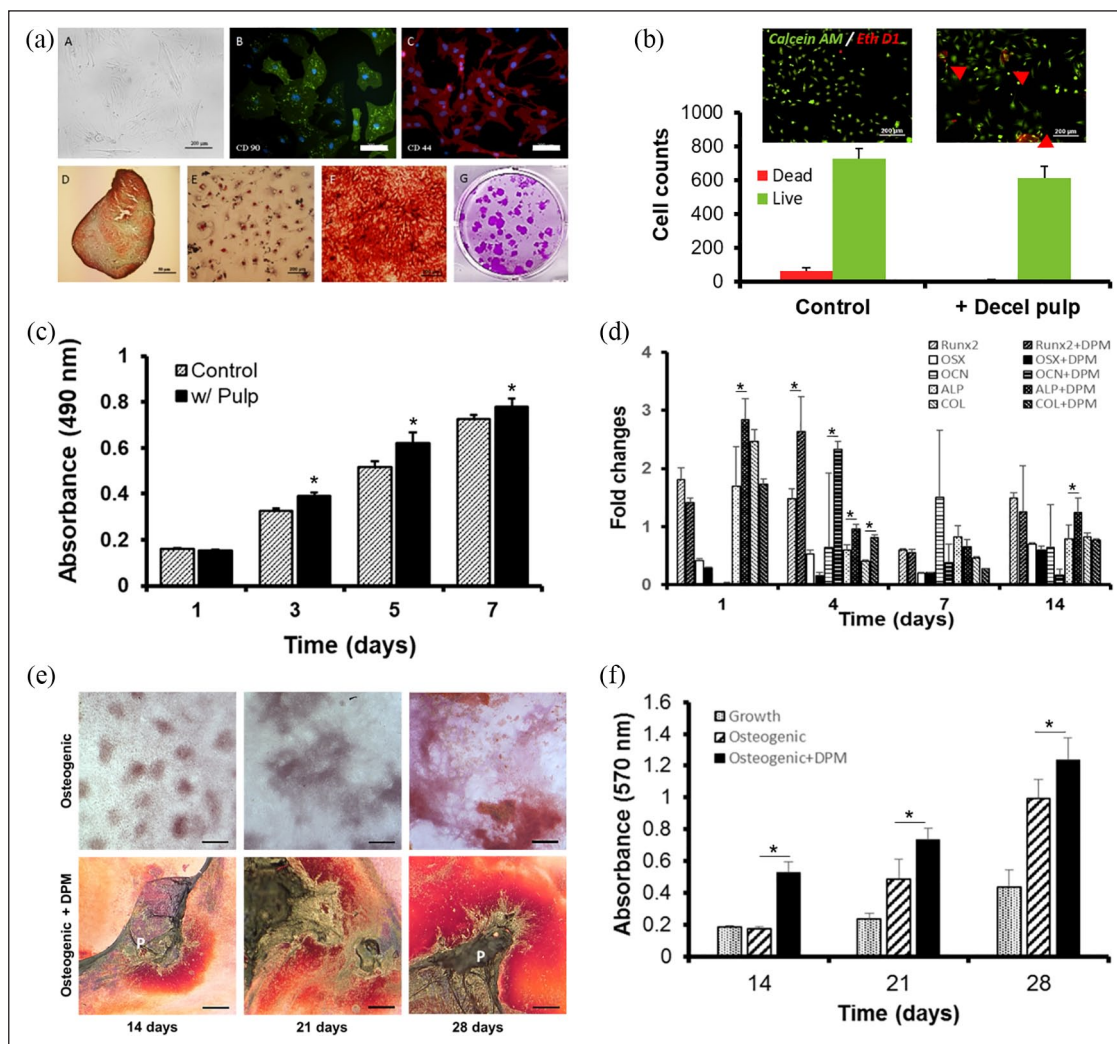
Figure 4. Characterization of MSCs isolated from rat bone marrow and their in vitro toxic, proliferative and osteogenic effect by DPM. MSCs were stained with CD44 and CD90, differentiated to chondrogenic, adipogenic, and osteogenic linage, and showed colony-forming capability (a), the Live/Dead Assay was performed to measure DPM's toxicity, with viable cells staining as green by Calcein-AM and dead cells staining as red by EtD-1 (b), MSC proliferation with and without DPM (control) was assessed by MTS on 1, 3, 5, and 7 days (c), the osteogenic gene expression was evaluated by real-time PCR analysis after culturing with and without DPM. All genes were normalized with GAPDH expression (d), microscopic images of mineralization by MSCs with and without DPM at 14, 21, and 28 days under osteogenic induction media (scale bar: 50 μm) (e), and CPC extraction of Alizarin Red S–stain was quantified by measuring the absorbance at 570 nm (f).

bound on the calcium nodules after 14, 21, and 28 days of osteogenic differentiation. Mineral nodules in the MSCs without DPM appeared after 14 days of osteogenic differentiation and increased over time up to 28 days (Figure 4(e)). Differentiation of MSCs with DPM powder resulted in significantly higher mineralization (0.53 ± 0.07 and 0.72 ± 0.06) than the MSCs without DPM (0.19 ± 0.01 and 0.48 ± 0.12), as indicated by ARS staining on day 14 and 21, respectively (*$p < 0.05$). DPM powder did not induced MSC's mineralization under growth media (data not shown). The level of mineralization reached 1.21 ± 0.14 in the MSCs with DPM powder group and 0.97 ± 0.12 in the MSCs only group by day 28 under osteogenic differentiation conditions (*$p < 0.05$) (Figure 4(f)).

MicroCT analysis

From the reconstructed MicroCT image (Figure 5(a)), the newly formed bone volume was calculated to be $5.57 \pm 1.43 \, mm^3$ in the DPM group with the MSCs and $0.78 \pm 0.38 \, mm^3$ in the DPM group without MSCs (Figure 5(b)). Most of the mineralized pulp merged with the surrounding host bone and some of them were observed at the center of defect, bridging mineralized pulps. The defect areas covered with the newly formed bone were $49.7 \pm 8.21\%$ in the DPM group with the MSCs and $0.12 \pm 0.32\%$ in the DPM group without MSCs (Figure 5(c)). Overall, the MSCs with DPM had greater volume and percentage of bone regeneration in the defect site versus DPM only.
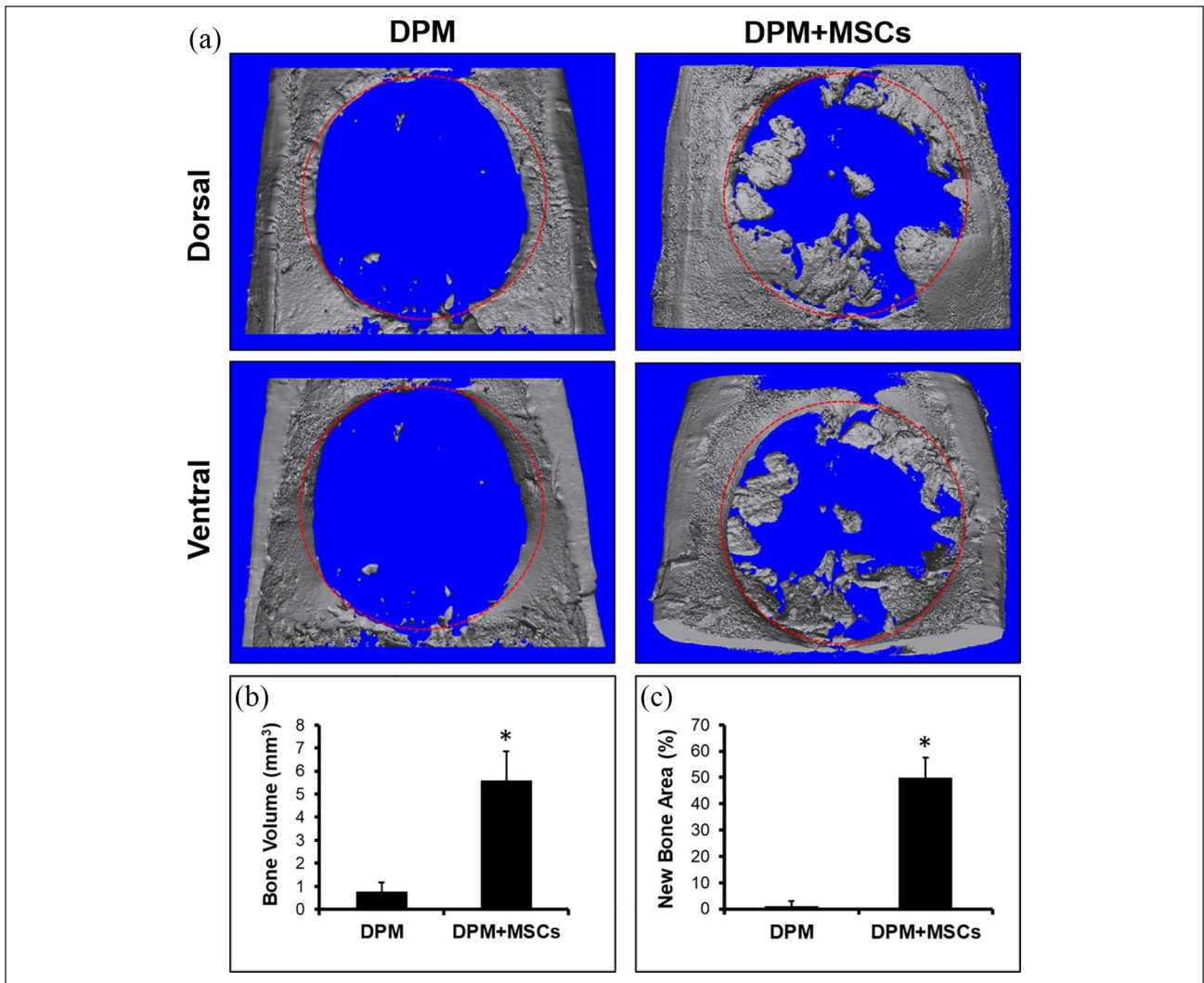
Figure 5. Micro-CT images of explanted calvaria containing critical sized defect after 12 weeks of implantation with DPM versus DPM seeded with MSCs (a), both bone volume (b), and new bone area (c) were calculated using Image J software. Red circle: defect site (8 mm in diameter). $n = 4$, $*p < 0.05$.

EDX and histological analysis

EDX analysis was assessed to quantify newly formed bone matrix of the MSCs with DPM, DPM only and calvaria served as control (Figure 6(b)). The atomic percentages of calcium were $17.7 \pm 1.41\%$, $31.1 \pm 1.43\%$, and 0% for calvaria, MSCs with DPM, and DPM only, respectively. For the phosphate, the atomic percentage were $8.45 \pm 0.77\%$, $13.7 \pm 0.96\%$, and 0% for calvaria, MSCs with DPM, and DPM only, respectively. The EDX results showed that the mineralized tissue in MSCs with DPM group preserved mineralized tissue with a Ca/P ratio of 2.27 in comparison with Ca/P ratio of 2.0 in calvaria group.

H&E histological section revealed mostly fibrous connective tissues from the DPM filling the calvaria defect site when only DPM was implanted. There was a lack of mineralized tissue like the host bone tissue, which stain darker due to the presence of bone cells in

lacuna (Figure 6(a)). Contrarily, DPM with MSCs successfully regenerated mineralized tissue that is similar to the natural calvaria in some parts of the defect. The transitional areas between the DPM and the newly mineralized tissue could be detected in the DPM+MSC group, unlike the DPM only group (Figure 6(a)). Further analysis using sections stained with Masson's trichrome showed newly formed collagen fibers, which are the platform for the mineralization, for the DPM with MSCs group (Figure 6(a)).

Assessment of vascularized new bone in CSD

After complete decellularization, the trace of blood vessels was observed in both new bone group regenerated with DPM and NPM group. The cross-sectional view of the vessels at each group of NPM, DPM, calvaria, and newly
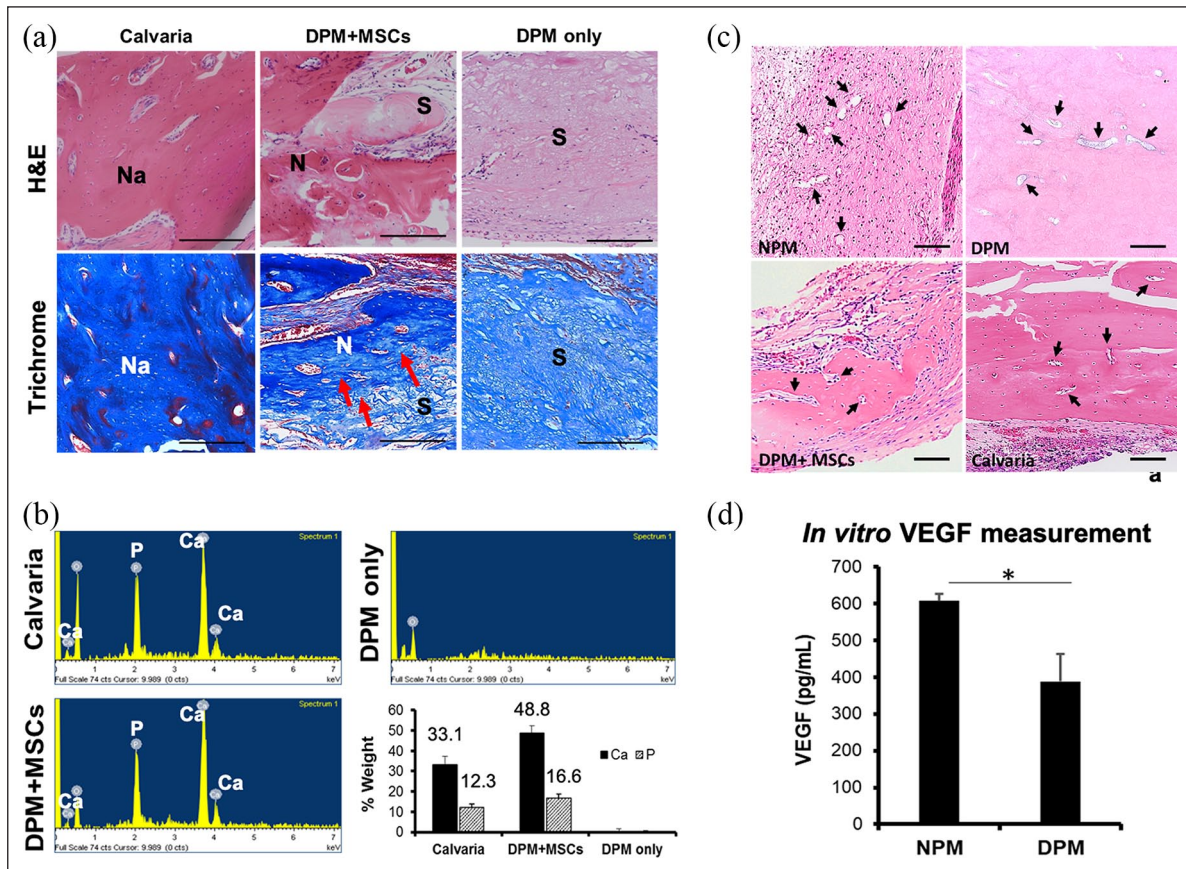
Figure 6. Evaluation of pulp matrices after in vivo biomineralization after 12 weeks of implantation in the CSD. H&E staining showed overall newly formed tissues in the medial-sagittal area on the defect site regenerated with DPM + MSCs, DPM, and calvaria, respectively. Trichrome staining revealed transition from pulp matrices to new bony collagen matrices, represented by the blue color (red arrows), Na: natural bone, N: newly formed bone, and S: DPM scaffold (a). EDX analysis for calcium and phosphate composition on three randomly selected areas on the CSD sites in each group (b), histological assessment of the vascular trait of newly formed bone with DPM + MSCs compared to calvaria, DPM, and NPM. Black arrows indicate vasculature trace (c), and in vitro measurement of vascular endothelial cell growth factor (VEGF) in both NPM and DPM (d).

formed bone using MSCs and DPM were visualized by H&E staining and listed in Figure 6(c). After Decellularization, residual VEGF could be detected using ELISA method, and was indicated to be 607.1 ± 18.7 and 387.9 ± 74.8 pg/ml for NPM and DPM, respectively. There was a significant loss of VEGF after decellularization process (Figure 6(d)).

Discussion

Natural bone substitutes, such as DecBM, have been demonstrating promising results in bone regeneration and seem to have the potential to become an ideal graft in clinical applications.[7,21] However, DecBM is not the optimal bone scaffold material in TE application as its compact structure of organic and inorganic matrices limit cell migration. Conversely, DPM, which has not been explored as extensively yet, seems to have less of DecBM's limitations and has the potential to be an

effective bone scaffold candidate. There are several important advantages to utilizing DPM for bone scaffold: there is an enormous supply of extracted teeth from which pulps can be collected; the method to prepare scaffold with pulp tissue is relatively easier than with other decellularized tissues; and the pulp contains ECM which improve cell seeding process by promoting infiltration and attachment. Additionally, DPM can be easily combined with other types of bone scaffold materials to increase the scaffold mechanical strength. Among all, the crucial advantage comes from DPM's ability to emulate the innate microenvironment for in vivo cellular homeostasis by providing space for cell anchorage and regulating cellular survival, proliferation, and differentiation via its proteins. Additionally, the collagen in DPM can interact with the seeded MSCs to promote organized biomineralization within and around collagen fibrils. Such qualities of DPM make it an outstanding candidate scaffold for bone regeneration.

Various analyses were conducted to ensure that none of the critical properties of DPM were altered by the decellularization process. Total collagen content, which is closely associated with the connective tissue's mechanical properties, was found to be not significantly different between DPM and NPM, confirming that decellularization had no effect on DPM's mechanical strength. Protein analysis showed a significant decrease in soluble protein levels after decellularization, possibly due to the loss of cellular components, soluble growth factors, and other proteins to the decellularization solutions. However, the lost soluble proteins are expected to be restored by the seeded MSCs. Overall, the DPM retained a majority of its structural composition and integrity, indicating its retained ability to facilitate cell retention

Preceding MSC seeding in DPM, we examined its cytotoxicity by culturing MSCs with DPM powder and performing a Live and Dead cell assay. While there were more deaths in MSCs with DPM, which might have been caused by direct contact with DPM, such result was insignificant compared to the survival rate of MSCs with DPM. Animal study further supported the non-toxicity of the DPM. Three months after implanting DPM, there was no sign of necrosis on the brain or other surrounding tissues during harvesting time. Overall, DPM was proven to be non-cytotoxic against MSCs and to be biocompatible in vivo.

In tissue engineering, cell-seeding has generally always been a challenge because of the difficulty in getting deep cell infiltration into the scaffold. However, pulp has similar ECM as other loose connective tissues. The major ECM component is collagen type I, and there is also a high amount of fibronectin and proteoglycan. The negatively charged sulfates in the glycosaminoglycan chains of the proteoglycans make the pulp heavily hydrated.[22] In terms of cell-seeding capability, this biochemical characteristic of pulp ECM can facilitate cell infiltration into the DPM and cell attachment to fibronectin and collagen. Effective infiltration was evident by the amount of mineralization and success of bone regeneration.

Overall, MSCs play a key role in bone regeneration, especially when DPM is used as a scaffold material, and our results confirmed this as DPM without seeded MSCs did not form any mineralized tissue whereas DPM with seeded cells induced mineralized pulp tissue in the rat CSD after 3 months. As a result, the EDX results of mineralized pulp showed the Ca:P ratio of 2.27 ± 1.47, which is higher than the 2.09 ± 1.81 ratio seen in calvarial bone. In physiological environment, osteoblasts and osteoclasts form and resorb bone by orchestrating signals from each cell and allow remodeling process to occur for bone homeostasis. If only osteoblasts are present, then such balancing effect may be missing and the newly regenerated bone may differ from the natural bone. However, the EDX analysis demonstrated that the osteogenically differentiated

MSCs in DPM could form mineralized bone-like tissue that is similar in ratios of the key elements as the natural calvarial bone. The higher Ca:P ratio in newly formed bone is likely to be adjusted by the remodeling process over time.

When repairing of critical bone defects, vascularization is one of the crucial factors as vessels supply essential components for bone formation.[23,24] In order to promote osteogenesis and vascularization, co-seeding endothelial cells with MSCs in the scaffold has been recommended in the previous research.[25]

Signs of vascularization have been observed in the newly formed bone tissue, and it is possible that vascularization has had an influence on the osteogenic effect on MSCs. Pulp is a highly vascularized organ,[26] and therefore there are endothelial cells that produce VEGF, a signal protein that stimulates blood vessels formation.[27] Such stimulation could have been intensified by the synergistic functionality of fibronectin and DPM. All these factors together could have led to the enhanced vascularization and, as a result, induction of new bone formation.[19]

Although the DPM may have positive effects on bone regeneration, no report of DPM utilization as a scaffold to regenerate bone tissue has yet been found. We detected and compared the amount of residual VEGF in the DPM and in fresh NPM. It is possible that DPM, which contains VEGF, have promoted the migration of host endothelial (or endothelial progenitor) cells and eventual vascularization in vivo. However, there has been no report about the direct cellular effects of the residual growth factors in the decellularized tissue, and it is still uncertain whether the bioactive molecules in the decellularized matrices directly stimulate bone cells for bone regeneration or whether the structural environment of decellularized matrices physically drives tissue regeneration by supporting cells. Nonetheless, our in vitro study further showed that DPM had an effect on cellular growth, osteogenic gene expression, and mineralization after culturing with MSCs, ultimately gaining mechanical integrity throughout bone regeneration. According to the study by Zhao et al., implantation of Stromal vascular fraction cells (SVFs) into acellular bladder scaffold could not only promote angiogenesis, but also increase the survival rate of the construct by the effect of pro-angiogenic factors from SVFs during bladder regeneration. In the future study, this concept can be applied to induce bone regeneration by promoting angiogenesis using proangiogenic factors.[28]

The downside of DPM as bone scaffold is the absence of initial mechanical strength to function as a nature bone. Unlike most bone scaffold that have high mechanical strengths to protect vital organ or to provide initial stability on the load bearing area, DPM has a mechanical strength that is similar to that of collagen sponge. Therefore, supportive techniques or devices will be necessary to protect

the defect site until it is completely repaired with new bone. Mixing DPM with other type of hard materials to fabricate a composite bone scaffold can be a potential solution. With the enhanced mechanical strength, the composite bone scaffold will be able to demonstrate outstanding bone regeneration capability with accelerated defect healing even at load bearing areas.

Although DPM show potential to induce biomineralization, the size of the tissue that can be regenerated by the individual pulp is quite small. For the application for larger bone defects, it is necessary to explore ways to fabricate larger integrated scaffolds that fit the defect site and effectively regenerate bone by providing sites for stem cells to anchor. Development of a more comprehensive fabrication technology that allows for flexibility in sizing and controllability of porous structure will improve the therapeutic application of DPM to repair even large bone defects.

ORCID iDs

Dong Joon Lee [iD] https://orcid.org/0000-0002-9284-0773

Hae Won Shin [iD] https://orcid.org/0000-0001-6400-6100

References

1. Johari B, Kadivar M, Lak S, et al. Osteoblast-seeded bioglass/gelatin nanocomposite: a promising bone substitute in critical-size calvarial defect repair in rat. *Int J Artif Organs* 2016; 39(10): 524–533.
2. Yassin MA, Leknes KN, Pedersen TO, et al. Cell seeding density is a critical determinant for copolymer scaffolds-induced bone regeneration, *J Biomed Mater Res A* 2015; 103(11): 3649–3658.
3. Fröhlich M, Grayson WL, Wan LQ, et al. Tissue engineered bone grafts: biological requirements, tissue culture and clinical relevance. *Curr Stem Cell Res Ther* 2008; 3(4): 254–264.
4. Oryan A, Kamali A, Moshiri A, et al. Role of mesenchymal stem cells in bone regenerative medicine: what is the evidence? *Cells Tissues Organs* 2017; 204(2): 59–83.
5. Marolt Presen D, Traweger A, Gimona M, et al. Mesenchymal stromal cell-based bone regeneration therapies: from cell transplantation and tissue engineering to therapeutic secretomes and extracellular vesicles. *Front Bioeng Biotechnol* 2019; 7: 352.
6. Cheng CW, Solorio LD and Alsberg E. Decellularized tissue and cell-derived extracellular matrices as scaffolds for orthopaedic tissue engineering. *Biotechnol Adv* 2014; 32(2): 462–484.
7. Chen G and Lv Y. Decellularized bone matrix scaffold for bone regeneration. *Methods Mol Biol* 2018; 1577: 239–254.
8. Lee DJ, Padilla R, Zhang H, et al. Biological assessment of a calcium silicate incorporated hydroxyapatite-gelatin nanocomposite: a comparison to decellularized bone matrix. *Biomed Res Int* 2014; 2014: 837524.
9. Song JS, Takimoto K, Jeon M, et al. Decellularized human dental pulp as a scaffold for regenerative endodontics. *J Dent Res* 2017; 96(6): 640–646.
10. Hu L, Gao Z, Xu J, et al. Decellularized swine dental pulp as a bioscaffold for pulp regeneration. *Biomed Res Int* 2017; 2017: 9342714.
11. Traphagen SB, Fourligas N, Xylas J, et al. Characterization of natural, decellularized and reseeded porcine tooth bud matrices. *Biomaterials* 2012; 33(21): 5287–5296.
12. Goldberg M and Smith AJ. Cells and extracellular matrices of dentin and pulp: a biological basis for repair and tissue engineering. *Crit Rev Oral Biol Med* 2004; 15(1): 13–27.
13. Benders KE, van Weeren PR, Badylak SF, et al. Extracellular matrix scaffolds for cartilage and bone regeneration. *Trends Biotechnol* 2013; 31(3): 169–176.
14. Sangkert S, Meesane J, Kamonmattayakul S, et al. Modified silk fibroin scaffolds with collagen/decellularized pulp for bone tissue engineering in cleft palate: morphological structures and biofunctionalities. *Mater Sci Eng* 2016; 58: 1138–1149.
15. Jung C, Kim S, Sun T, et al. Pulp-dentin regeneration: current approaches and challenges. *J Tissue Eng* 2019; 10: 2041731418819263:
16. Hargreaves KM, Cohen S and Berman LH. *Cohen's pathways of the pulp*. 10th ed. St. Louis, Mo: Mosby Elsevier, 2011.
17. Sangkert S, Kamonmattayakul S, Chai WL, et al. Modified porous scaffolds of silk fibroin with mimicked microenvironment based on decellularized pulp/fibronectin for designed performance biomaterials in maxillofacial bone defect. *J Biomed Mater Res A* 2017; 105(6): 1624–1636.
18. Thai TH, Nuntanaranont T, Kamolmatyakul S, et al. In vivo evaluation of modified silk fibroin scaffolds with a mimicked microenvironment of fibronectin/decellularized pulp tissue for maxillofacial surgery. *Biomed Mater* 2017; 13(1): 015009.
19. Lee DJ, Lee YT, Zou R, et al. Polydopamine-laced biomimetic material stimulation of bone marrow derived mesenchymal stem cells to promote osteogenic effects. *Sci Rep* 2017; 7(1): 12984.
20. Rasband WS. and ImageJ, U. S. Bethesda, MD: National Institutes of Health, https://imagej.nih.gov/ij/ (1997-2018).
21. Lee DJ, Diachina S, Lee YT, et al. Decellularized bone matrix grafts for calvaria regeneration. *J Tissue Eng* 2016; 7: 2041731416680306.

22. Sloan AJ. Stem cell biology and tissue engineering in dental sciences. In: A Vishwakarma, P Sharpe, S Shi, et al. (eds) *Biology of the dentin-pulp complex*. London: Academic Press, 2015, pp.371–378.

23. Salvay DM, Rives CB, Zhang X, et al. Extracellular matrix protein-coated scaffolds promote the reversal of diabetes after extrahepatic islet transplantation. *Transplantation* 2008; 85(10): 1456–1464.

24. Tian T, Zhang T, Lin Y, et al. Vascularization in craniofacial bone tissue engineering. *J Dent Res* 2018; 97(9): 969–976.

25. Liu X, Chen W, Zhang C, et al. Co-seeding human endothelial cells with human-induced pluripotent stem cell-derived mesenchymal stem cells on calcium phosphate scaffold enhances osteogenesis and vascularization in rats. *Tissue Eng Part A* 2017; 23: 546–555.

26. Hong S, Lee J, Kim JM, et al. 3D cellular visualization of intact mouse tooth using optical clearing without decalcification. *Int J Oral Sci* 2019; 11(3): 25.

27. Feng L, Wu H, Wang D, et al. Effects of vascular endothelial growth factor 165 on bone tissue engineering. *PLoS One* 2013; 8(12): e82945.

28. Zhao F, Zhou L, Liu J, et al. Construction of a vascularized bladder with autologous adipose-derived stromal vascular fraction cells combined with bladder acellular matrix via tissue engineering. *J Tissue Eng* 2019; 10: 2041731419891256.